POTENTIAL ANALYSIS FOR SIMULTANEOUS FORMATION FLIGHT DEPARTURES

G. Schmitz[1], T. Marks[2], F. Linke[2]
[1]German Aerospace Center (DLR), Institute of Flight Systems, Braunschweig
[2]German Aerospace Center (DLR), Air Transportation Systems, Hamburg

Gregor.Schmitz@dlr.de
Tobias.Marks@dlr.de
Florian.Linke@dlr.de

Abstract

The climate change is one of the most urgent challenges of today with aviation being one of the major contributors. It is, therefore, essential to decrease the climate impact of aviation by technical and operational means. One promising operational procedure to significantly reduce the fuel consumption and thus the emissions of an aircraft is the fuel-saving formation flight that is also called aircraft wake-surfing for efficiency (AWSE). However, the coordination of formation build-up for aircraft originating from different airports can be challenging due to timing and routing issues. Two formation partners departing from the same airport in contrast can be expected to achieve substantial benefits as the joint flight time can be maximized and detours can be minimized. Therefore, within this paper potential two-aircraft formation candidates scheduled for departure from the same airport within a certain time interval will be identified by means of filtering an existing global flight schedule. Based on these data the potential of an airport to conduct simultaneous formation flight departures will be assessed. Furthermore, it will be analyzed how this potential changes if time offsets between the departures of the formation members are accepted. In addition, the fuel-saving benefits of the identified formations will be estimated by modeling the formation routes and by assessment with advanced surrogate models. It will be shown that, although today's flight schedules are not optimized for AWSE, a potential for simultaneous departures especially at the big hub airports exists that can lead to substantial fuel savings.

Keywords: wake-surfing, formation flight, fuel savings, airport potential

ABBREVIATIONS

ADI	Airport Data Intelligence
AWSE	Aircraft Wake-Surfing for Efficiency
BADA	Base of Aircraft Data
CTOT	Calculated Take-Off Time
DLR	Deutsches Zentrum für Luft- und Raumfahrt (German Aerospace Center)
FC	Formation Candidate
FCA	Formation Cruise Altitude
FCM	Formation Cruise Mach number
FEP	Formation End Point
FSP	Formation Start Point
IATA	International Air Transport Association
NASA	National Aeronautics and Space Administration
RSP	Rendezvous Start Point
SEP	Separation End Point
TOC	Top of Climb
TOD	Top of Descent

NOMENCLATURE

FCA	$[ft]$	Formation cruise altitude
FCM	$[-]$	Formation cruise Mach number
g	$\left[\frac{m}{s^2}\right]$	Gravitational acceleration
k	$[-]$	Number of scheduled flights (of an airport)
lf	$[-]$	Load factor
n	$[-]$	Number of formation candidates (of an airport)
N	$[-]$	Number of formations (formation flight schedule of an airport)
R	$[m]$	Turn radius
S	$[NM]$	Route length
V	$\left[\frac{m}{s}\right]$	Cruise speed
μ	$[-]$	Airport formation flight classification number
ξ	$[-]$	Relative route length
σ	$[-]$	Lateral metric describing the relative detour
φ	$[°]$	Bank angle
ΔF	$[t]$	Estimated fuel savings
ΔT	$[min]$	Departure time offset (filter criteria)
$\Delta\psi$	$[°]$	Difference between azimuth angles (origin to both destination airports) (filter criteria)

a	Approach segment
ap	Airport
av	Average (all airports of a scenario)
$awse$	AWSE mission
b	Beneficial segment
c	Continuation segment
fc	Formation candidate
fw	Follower
ld	Leader
ref	Reference mission
tot	Sum (all airports of a scenario)

1. INTRODUCTION

As early as 1914, Wieselsberger [1] discovered that flying in formation allows migrating birds to reduce the amount of energy needed during flight. Thus, they can extend their range drastically. Further studies on the flight behavior of birds [2, 3] developed general understanding of the aerodynamic principles, and the idea of transferring the concept of formation flight to man-made aircraft was born. Theoretical analyses of fuel-saving formation flight, that is also called aircraft wake-surfing for efficiency (AWSE), promise significant fuel savings and consequently reduced emissions by introducing this concept into the air transportation system. Flight experiments performed with

doi:10.25967/530061

research aircraft and modified fighter jets showed that the theoretical fuel savings of up to 18 % can be achieved in practice [4, 5]. Further flight tests conducted by NASA demonstrated a substantial fuel saving potential even with an enlarged longitudinal spacing between both aircraft [6]. However, the documented fuel savings of these experimental test flights may not be directly transferable to the overall air transportation system due to inefficiencies caused by detours, different aircraft types and loading conditions, or adjusted flight speeds.

For this reason, numerous studies have assessed achievable fuel savings in real-world scenarios on the basis of existing global flight schedules [7-12]. However, the integration of formation flight into the air transportation system is subject to risks and challenges associated with unforeseen events such as bad weather conditions, technical problems or limited airport capacity. These circumstances may lead to delay of one aircraft, while the other aircraft is already on the way to meet up at a certain rendezvous point. As a consequence, holding patterns, re-routings, or speed adjustments are necessary to compensate asynchrony in terms of arrival time at the rendezvous point reducing the overall mission benefits. Accurate timing is essential for the successful operation of pre-flight planned formation flights and determines the achievable fuel savings in daily operation [13].

One way to reduce the negative impact of delay is to assign only those aircraft to a formation that depart from the same airport. Consequently, there is no complex coordination of aircraft departing with various time offsets from different airports to meet at a rendezvous point simultaneously. Less dependency on flight schedules of other airports and short communication paths at one airport allow for a more flexible response to ground delay. Possible mitigation measures are to assign delays to aircraft while still on ground or to identify alternative formation members. If the delay cannot be compensated, the formations can be cancelled to operate individual flights with minimum delay and detours.

Another positive side effect of operating formations from the same airport can be the omission of detours prior to the start of the fuel-saving formation flight phase. Furthermore, shifting the beneficial flight phase towards the beginning of the entire flight route makes the formation flight more efficient [14].

Unlike previously mentioned studies, this study, therefore, deals with the identification of formation candidates (FCs) departing from the same airport. Potential fuel savings are assessed on the basis of an existing global flight schedule.

2. APPROACH

2.1. General approach

Figure 1 shows the general approach as followed in this study. In a first step the global flight schedule data (Sabre Airport Data Intelligence database (ADI data)) [15] is processed and separated into local flight schedules of each airport. Based on these local flight schedules FCs of each airport are identified in a multistage filtering process. An FC is defined as a set of two flights assigned to join a two-aircraft formation. Furthermore, each flight, which is also referred to as formation member, is clearly assigned to its position, which can be either leader or follower. Thus, each set of two flights counts as two FCs by means of varying the position. The airport potential to conduct simultaneous formation flight departures is then assessed by means of analyzing the number of resulting FCs of an airport. Moreover, the filter criterion ΔT is varied to analyze how the potential changes if deviations from the flight schedule are permitted. ΔT is defined as the permitted time offset between the scheduled departure times of both formation members.

In the next step the flight routes of all FCs are modelled and the fuel savings are assessed using advanced surrogate models according to Marks et al. [14, 16, 17].

From these FCs, formation flight schedules of each airport that assign each flight uniquely to one formation are created. Thus, a more realistic estimation of the achievable fuel savings is obtained, although the effect of delay caused by detours on the fleet and aircraft circulation planning is neglected.

A second airport analysis on the basis of these optimized flight schedules determines the airport potential with respect to the fuel savings. These fuel savings, summed up over all airports, reveal the worldwide fuel saving potential.

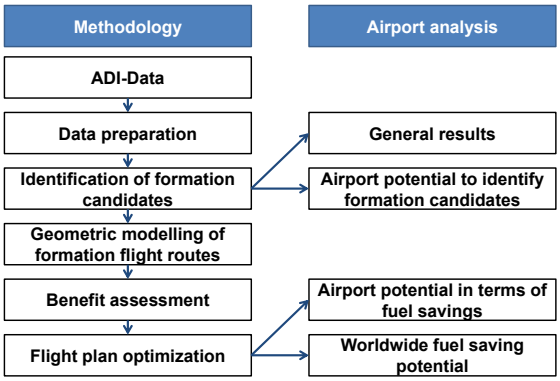

Figure 1: General approach

2.2. Assumptions

Concerning the conduction and modelling of formation flight several assumptions are underlying the study presented in this paper.

As it is most likely to start with the simplest implementation of AWSE into the existing air transportation system, only two-aircraft formations without positional changes are considered in this study. The formation cruise altitude (FCA) and the cruise speed are considered to be constant during the formation. The cruise speed is specified as a formation cruise Mach number (FCM). FCA and FCM are chosen as the lower cruise altitude and cruise Mach number of both formation members according to the BADA flight performance database version 4 from EUROCONTROL [18], which is used for all calculations related to the flight performance of an aircraft.

Another input parameter of the surrogate models is the load factor lf that is defined as the ratio of the transported payload to the maximum payload. It is set to an average value of 0.78 as determined by IATA [19].

Furthermore, the study is limited to long-range aircraft with flight routes of at least 1000 km, because long-haul flights can be expected to benefit most from AWSE.

For the modelling of the formation flight routes it is assumed that ground handling processes of both formation members at the same airport can be either completed simultaneously or there is the opportunity to wait for each other at the ground in order to enable simultaneous departures in the desired order.

Following the definition of the calculated take-off time (CTOT) according to EUROCONTROL [20], which is defined by a time and a tolerance of -5 min and +10 min during which period a flight is expected to take-off, the upper limit for the time offset ΔT is set to 10 min. Thus, in comparison to simultaneously scheduled departures a larger candidate pool may lead to more promising formations, whereas the departure times stay within the permitted deviation from the flight schedule. Within the first analysis of the airport potential, ΔT is varied from 0 min to 10 min in steps of 5 min, which corresponds to the accuracy of the departure times.
Following the heuristic filter criteria of [10], 30° is chosen as an appropriate $\Delta\psi$ limit in order to ensure similar flight directions. $\Delta\psi$ is defined as the angular difference between great circle flight tracks to the destinations of both formation members measured from the origin airport. It is always the minor angle.

3. METHODS

3.1. Data preparation

The identification of FCs is based on a global flight schedule of October 2014 taken from the Sabre Airport Data Intelligence (ADI) database [15]. The original database provides a list of recurring flights specified by:

- Origin airport and local departure time
- Destination airport and local arrival time
- Operating airline
- Aircraft type
- Weekday of flight operation
- Day and time period of flight operation
- Number of operated flights within the time period

A flight schedule that lists every single flight, also specifying the explicit date and departure time of recurring flights operated under the same flight number, was created using these data. This global flight schedule was subsequently filtered by aircraft types in order to reduce the calculation effort. In a next step, the remaining flight schedule was split up into local flight schedules of each airport.

3.2. Identification of FCs

The identification of FCs at an airport is based on binary matrices of the size $k \times k$ assigning all flights k of an airport to a certain row and column with the help of a unique flight-ID. Thereby, each entry of the matrix represents a combination of two flights. The row index represents the leader flight-ID, whereas the column index represents the follower flight-ID, such that both assignments of a flight to either the leader position or the follower position of a formation are considered in the matrix. Entries along the main diagonal are ignored and marked with zero, since they would represent formations of flights with themselves. In a multistage filtering process the flight combinations are analyzed and marked respectively. Promising flight combinations are marked with one. Entries that did not pass a filter step are not considered within the further filtering process and are marked with zero. The filtering steps are shortly described in the following.

Departure time offset
The choice of the same origin airport in connection with the flights being sorted by departure time allows starting the filtering process with a zero matrix, since suitable formation pairs in terms of departure time offset are all located around the main diagonal. By means of a supporting table listing all departure times and related flight-IDs of flights scheduled within the permitted time interval, only flight pairs that pass the time offset criterion ΔT are analyzed and marked with one. Consequently, the number of flight pairs to be checked is reduced drastically compared to the combinatorial set of all flights.

Flight direction
It is obvious that flights with opposite or too diverse flight directions are not suitable to conduct a formation flight. For this reason, the difference of azimuth $\Delta\psi$ represents the second filter criteria, which has to be below the limit value of 30°.

Aircraft type combination
The third criteria being checked is the aircraft type combination. Besides too diverse cruising speeds or altitudes that may prevent aircraft pairs from flying in formation, restrictions on the position within the formation are conceivable. Within this study there are no restrictions made here, because only long-haul aircraft types with similar flight characteristics are analyzed.

Scenario filters
The fact that only the follower harvests the AWSE benefits, whereas in most cases the leader has additional expenses due to detours, necessitates a cost sharing model. The implementation of formation flight within the same airline provides an opportunity to avoid the cost sharing question.
Alternatively, flights from members of the same airline alliance can be assigned to formations to exploit a broader route network. Furthermore, the analysis of formations between flights that have origin and destination in common can be of particular interest because those formations imply least need to adjust the existing flight schedule.
In order to analyze the impact of these scenarios on both the number of formations at each airport and the achievable fuel savings, the filter method enables to take into account the following filter criteria within a second filter stage:

- Minimum flight route
- Membership in a particular airline
- Membership in a particular airline alliance
- Common destination
- Limitation to particular aircraft types

3.3. Geometric modelling of formation flight routes

For all FCs that have been identified by the previous steps, valid formation flight routes are determined in order to estimate achievable fuel savings.

3.3.1. Lateral flight track

Figure 2 depicts a simplified scheme of the lateral flight track of both formation members, pointing out significant waypoints and flight segments used to describe a formation. In order to simplify the calculations, flight routes

are modelled as the shortest connection along great circle flight paths between these characteristic waypoints.
Because in most cases the destination airport of leader and follower is different, the flight routes of their individual flight mission (dashed lines), directly connecting origin airport and respective destination airport, span a triangle with the inner angle $\Delta\psi$ at the origin airport. In order to get a shared flight route both aircraft need to deviate from their individual flight routes, which are referred to as reference flight routes S_{ref}.

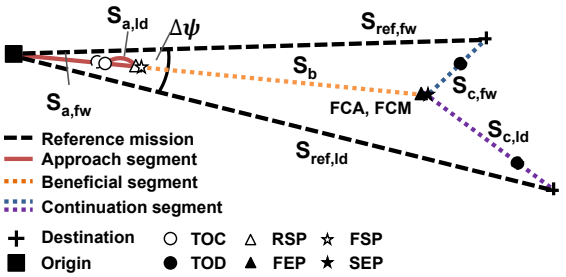

Figure 2: Schematic illustration of the lateral flight tracks

The formation flight mission (S_{awse}) typically consists of three main sections as specified by Marks et al. [14, 16, 17]. The approach segment S_a starts at the origin airport and ends at the formation start point (FSP). It also covers a rendezvous maneuver starting at the rendezvous start point (RSP) that initiates the transition to the beneficial segment S_b. This joint flight segment ends at the formation end point (FEP), where the aircraft start to separate. The separation phase is part of the continuation segment S_c and ends at the separation end point (SEP), where both aircraft have left the formation and continue to their destination airports.
In this study, it is assumed that leader and follower depart from the same origin airport and thus the approach segments of both aircraft overlap. Because not all airports have multiple independent runways and most airports with independent runways use them to operate departures independently of arrivals, it seems reasonable to suppose that both formation members need to depart sequentially.

Compensation of delay

It is very likely that safety-relevant wake vortex separation between two departures, different flight performances due to different aircraft take-off weights or engine types, and other operational or safety-related factors will result in a longitudinal offset between both aircraft positions at the time, when both aircraft have reached the formation cruise altitude. This offset can be reduced by several means in order to establish a stable, parallel flight prior to the rendezvous maneuver. It is assumed that the leader always departs first in order to avoid overtaking maneuvers. Speed adjustments or modified routings could allow the follower to catch up to the leader. Depending on airspace capacities, flight performances and safety regulations, these measures can be conducted either after reaching FCA, reducing the length of the joint flight segment, or already during the climb phase.
It is conceivable that such a catch-up maneuver is restricted to be conducted in predefined flight altitudes or airspace (e.g. above uninhabited terrain) in order to comply with safety concepts or to avoid interference with regular flights. Therefore, in this study existing regulatory restrictions with respect to aircraft separation are taken into account for the modeling of takeoff and climb segments in order to estimate the RSP position. It is assumed that the longitudinal offset at the time when both aircraft have reached the common FCA complies with the typical en-route radar separation of at least 5 NM [21]. As it is indicated in Figure 2, the routing of the leader is then modified by an additional detour, whereas the follower flies along the formation segment, which allows him to catch up to the leader. Speed adjustments are not considered here. In this way, the impact of longitudinal offsets between both formation members that may reduce the length of the joint flight segment is modelled in order to get a conservative and probably more realistic estimation of the achievable fuel savings. In addition, plots of all customized detours around one airport give an overview about the range of potential locations of formation built-up. Depending on the safety concept, this information may help to identify above mentioned predefined airspaces used for formation built-up, potential conflicts with other airports, or the opportunity to share such rendezvous airspace.

3.3.2. Vertical flight profile

Figure 3 depicts a simplified scheme of the vertical flight profile of both formation members pointing out all the characteristic waypoints that have been mentioned before. Both formation members depart from the same airport and climb to the common formation cruise altitude (FCA). At their top of climb (TOC) both formation members continue in level flight. After separation, both formation members may climb to an optimal cruise altitude depending on their remaining flight time and aircraft weight.
Information about the distances covered during climb and descent are used to determine the RSP and SEP positions. The top of descent (TOD) is only used to shift the SEP towards the RSP in case the descent flight phase coincides with the formation flight phase.

Estimation of TOC and TOD

The positions of TOC and TOD are determined by the climb and descent performance of the aircraft, which depends mainly on the aircraft weight. Within the BADA database, the load factor lf and the transported fuel, which scales with the length of the flight mission, affect the aircraft weight and thus the aircraft performance. The flight performance of the leader is calculated on the basis of the resulting formation flight route, whereas the follower flight performance is calculated on the basis of the reference mission, because it is assumed that the fuel savings do at least compensate detours. FCs with a formation flight route exceeding the range of the leader aircraft are not considered in the further assessment.

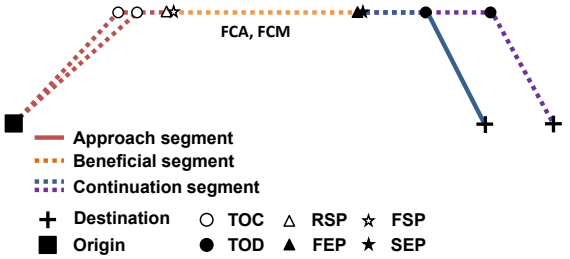

Figure 3: Schematic illustration of the vertical flight profile

Estimation of FEP and SEP location

In case both formation members have not only the origin airport but also the destination airport in common, the SEP is located on the great circle track between those airports and coincides with the TOD that is further away from the

destination airport. Otherwise, a geometric approach is used, which is based on the assumption that fuel consumption scales with the flight route. The SEP is determined by means of the Fermat point principle for spherical triangles [22] with the three airports being the corner points of the triangle such that the flight routes represent the geometrically shortest possible routes for both aircraft while ensuring a shared flight route to the SEP. The SEP position found in this way is then checked for conflicts with the TOD of both aircraft, because the formation cannot be maintained during the descent flight phase of one aircraft. If the SEP is located too close to or at one of the destination airports, the SEP is moved along the great circle path towards the origin airport until it coincides with the TOD.
The separation maneuver is assumed to be unproblematic and can be conducted easily by the follower either reducing speed or conducting a turn or descent maneuver. For this reason, within this study there is no distinction made between FEP and SEP.

Estimation of RSP location
In a first step, the travel distances of leader and follower at the time when both aircraft have reached the FCA are estimated using the flight performance models. The delayed departure due to separation of the follower aircraft is taken into account. In order to assess this delay, all considered aircraft were assigned to one of the six wake vortex categories as described in [23].
Mathematically, the difference of both distances travelled yields the offset that needs to be reduced to a longitudinal spacing that allows a safe and profitable implementation of AWSE. Because it is common practice to delay the departure of a following aircraft in case it would catch up to the previous aircraft [24], it is assumed that for safety reasons the offset between leader and follower is not less than the common radar separation of 5 NM, as the follower does not overtake or catch up to the leader during climb.
In order to assess the RSP position, it is assumed that the leader aircraft deviates from the direct flight track to the SEP, while the follower aircraft continues along the direct flight track. For this purpose a customized, arc-shaped detour is modelled that extends the leader flight track in comparison to the straight follower flight track by the offset length. Thus, neglecting wind, as in the entire study, and assuming a common cruise speed, the offset is reduced to a theoretical value of zero at the end of this detour maneuver. The resulting end point represents the RSP.
For simplicity reasons, two different detour shapes based on simple geometric considerations as shown in Figure 4 are used. These geometries allow customizing the detour length by variation of the length of the green colored straight flight sections. Option (a) begins with a turn changing the leader flight direction by 45°, whereas in option (b) the flight direction is changed by 90°. Because in option (b) the leader aircraft flies perpendicular to the follower flight track, an increase of the detour length does not affect the position of the RSP, because the additional length to the follower flight route (dashed line) is limited and depends only on the turn radius. The turn radius is determined according to Eq. (1) [25] with the gravitational acceleration g, cruise speed V and bank angle φ. In accordance with [24], it is assumed that in cruise flight the maximum bank angle φ should not exceed 25° in order to guarantee passenger comfort.

$$R = \frac{V^2}{g \tan \varphi} \tag{1}$$

The detour shape is chosen depending on the offset distance. At small offsets option (a) is used, whereas for larger offsets option (b) is implemented. However, the best measure is depending on several factors, such as airspace capacity, safety regulations, additional speed adjustments, or passenger acceptance.

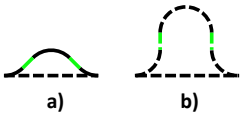

Figure 4: Detour shapes depending on the resulting offset

Estimation of FSP location
Assuming a stable, parallel flight of leader and follower at the RSP, according to Marks et al. [14, 16, 17] a rendezvous maneuver initiates the beneficial flight phase. Throughout this maneuver, communication channels may be set up and the follower positions itself at the outer side of the wake of the leader. Within this work, it is assumed that both aircraft cover a distance of about 30 km while conducting this maneuver corresponding to approximately 2 min of flight time. Thus, the FSP is assumed to be located 30 km downstream from the RSP.
$S_{a,fw}$ is given by the great circle distance between origin airport and FSP, whereas $S_{a,ld}$ is increased by the longitudinal offset due to the arc-shaped detour.

3.4. Benefit assessment

The benefit of each FC is assessed using surrogate models according to Marks et al. [14, 16, 17], which are briefly described below.
On the basis of parameter variations with an integrated software environment for numeric simulation of formation flights (MultiFly), Marks et al. derived surrogate models that allow an estimation of the formation benefits based on the formation route geometry and mission parameters. Thus, as pointed out in Eq. (2), the absolute fuel savings of a formation ΔF_{fc} can be estimated as a function of eleven parameters. The first seven parameters are characterized by the formation flight routes, as these have a large effect on the achievable fuel savings. Added to these parameters are the load factors (lf), FCA, and FCM.

$$\Delta F_{fc} = \begin{matrix} f(\sigma_{ld}, \sigma_{fw}, \xi_{b,ld}, \xi_{b,fw}, \xi_{a,ld}, \xi_{a,fw,\ldots} \\ S_{awse,ld}, lf_{ld}, lf_{fw}, FCA, FCM) \end{matrix} \tag{2}$$

The lateral metric σ describes the relative detour. ξ_a and ξ_b describe the relative length of the approach segment and of the beneficial segment according to Eqs. (3).

$$\sigma = \frac{S_{awse} - S_{ref}}{S_{ref}} \qquad \xi_a = \frac{S_a}{S_{awse}} \qquad \xi_b = \frac{S_b}{S_{awse}} \tag{3}$$

3.5. Flight plan optimization

In the previous step, the benefit of all FCs has been assessed. Both formation setups with respect to the position of each formation member, assignments of flights to multiple formations and formations with increased fuel consumption are included. In order to get a more realistic

estimation of the overall achievable fuel savings, an optimized formation flight schedule that assigns each flight only to one formation is required, because each aircraft can only attend one formation at a time. A simplified approach is used here.
First of all, all FCs with negative fuel savings are crossed out, because these FCs should prefer their individual flight missions. Next, the more efficient setup is chosen. Due to multiple assignments of flights to different formations, the choice of the best set of formations with respect to the overall fuel savings becomes a linear optimization problem, which has been solved using the MATLAB Optimization Toolbox. The candidate pool for the optimization of the flight schedule was identified at filter settings of $\Delta T = 10$ min and $\Delta\psi = 30°$.
Formation flight between aircraft with different destinations may lead to delay caused by detours. Consequently, the following missions cannot be operated according to the flight schedule anymore. Therefore, the operational implementation of formation flight into the air transportation system requires a flight schedule customized for formation flight. However, the present analysis is meant to assess the potential fuel savings based on an existing flight schedule and does not take into account planning of flight missions. Effects on fleet and aircraft circulation planning are neglected.

3.6. Airport analysis

At first, the potential to identify promising FCs that are characterized by similar flight directions of both formation members is analyzed for each airport solely based on the results of the multistage filtering process. The time offset criterion ΔT is varied to analyze how this potential changes if deviations from the flight schedule are allowed.
Because in general the number of scheduled flights increases the chance to identify two flights with similar flight directions, an airport formation flight classification number μ for the assessment of the airport potential is introduced according to Eq. (4). This classification number provides a better comparability between the potential of airports with very diverse numbers of scheduled flights, as it sets the number of formation candidates n in relation to the number of scheduled flights k.

$$\mu = \frac{n}{k} \tag{4}$$

The second analysis is based on the optimized flight schedules and evaluates the potential of an airport with respect to the fuel savings.

4. RESULTS

In this chapter the results of the studies will be presented. Generally, three scenarios were considered for the analysis of the airport potential:

- Scenario I: All formations
- Scenario II: Formations with common destination
- Scenario III: Formations of Star Alliance

The first two subchapters deal with the analysis how ΔT affects the number of FCs. In chapter 4.1 general results considering all airports will be presented followed by a more detailed comparison of the airport potential among the Top 10 airports in terms of μ in chapter 4.2. Because the fuel savings scale with the quality as well as with the quantity of formations, the focus of the further analysis is shifted to the number of formations in the formation flight schedule. Comparisons between the number of formations and related fuel savings among the Top 15 airports allow drawing conclusions about the average efficiency of formations among these airports in section 4.3. The last section presents the estimated worldwide fuel savings.

4.1. General results

The overall flight schedule contains 196677 long-haul flights from 446 airports within the considered time period of October 2014. Because the total number of scheduled flights at the airports varies between 1 and 8162 flights the number of FCs identified at each airport varies accordingly. Figure 5 to Figure 7 provide an overview about this variety for the three scenarios. The plots show the number of airports over the number of FCs.
Furthermore, the effect of an increased time offset ΔT is illustrated by using different colors. It is clearly visible that a larger allowed time offset results in an increase of the number of airports for that FCs can be identified as well as an increase of the number of FCs in total. Note that the horizontal axis uses a logarithmic scale. The number of FCs summed up over all airports as well as the arithmetic average is stated in the legend.

Scenario I – All formations
In the first scenario (Figure 5) without restrictions in the scenario filter settings, the number of formation airports varies between 105 and 159 depending on the time offset. Because over 93 % of all long-haul flights (183253 flights) are operated at these 159 airports, at the remaining 287 airports no FCs were found. The increase of the total number of FCs, when increasing ΔT from 0 min to 5 min or from 5 min to 10 min, is almost constant at about 76000 new candidates. However, with an increase of ΔT, airports with many scheduled flights show a stronger increase of FCs compared to those with less scheduled flights. This is likely to result from the nonlinear increase of the combinatorial possibilities to build up a formation. Furthermore, the larger candidate pool may provide alternative FCs in the event of delay.
It can be seen for all values of ΔT that roughly 20 % of all airports have less than 10 FCs, whereas the percentage of airports with more than 1000 FCs increases from 12 % to 21 % between $\Delta T = 0$ min and $\Delta T = 10$ min. A few airports have very high numbers of FCs of up to 20940. All three curves show a flattening of the gradient towards higher numbers of FCs.

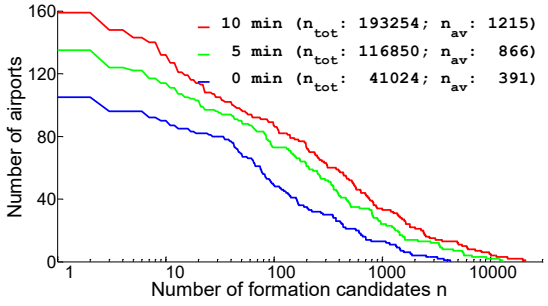

Figure 5: Number of airports over number of formation candidates depending on ΔT (Scenario I)

Scenario II – Common destination

The second scenario considers only formations that have a common destination. Thus, the number of FCs summed up over all airports is significantly reduced (Figure 6). There are only 2350 FCs at $\Delta T = 0$ min and 12802 FCs at $\Delta T = 10$ min. These values correspond to 5.7 % and 6.6 % of the FCs in scenario I. The number of airports with potential to conduct simultaneous formation flights is also reduced to 55, 78, and 94 depending on the time offset. The average number of FCs per airport is reduced to 11 % of the values for the same ΔT in scenario I. Although the maximum number of FCs ($\Delta T = 10$ min) is limited to 1300, the flattening of the gradient is still visible at higher numbers of FCs for all curves.

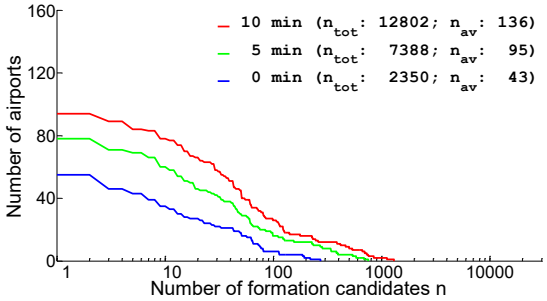

Figure 6: Number of airports over number of formation candidates depending on ΔT (Scenario II)

Scenario III – Star Alliance

30.6 % of all flights (60225 flights) are operated by a member of Star Alliance. These flights are distributed among 270 airports, but 46 airports operate more than 80 % of these flights. Thus, the limitation to formations with members that belong to the same airline alliance (Star Alliance is used as an example here) further decreases the number of airports compared to scenario II (Figure 7).

The cumulated number of FCs for each time offset is reduced to values between 15 % and 18 % of the related number in scenario I. However, the average number of FCs reaches at least 37.5 % of the related number in scenario I due to the reduced number of formation airports. This is consistent with the flatter gradient of the curves and the fact that few airports have high numbers of FCs of up to 4432.

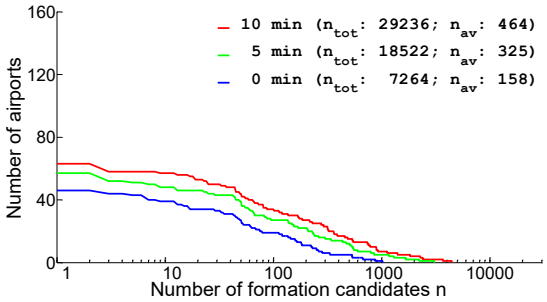

Figure 7: Number of airports over number of formation candidates depending on ΔT (Scenario III)

4.2. Airport potential to conduct simultaneous formation flight departures

Because it is not feasible to compare the potential of all airports, the following analysis focuses on the Top 10 airports of each scenario. The Top 10 airports are chosen on the basis of the classification number μ and for $\Delta T = 10$ min. Thus, the analysis also takes into account small airports with only few flights.

In Figure 8 to Figure 10 the formation flight classification number μ is plotted over the number of FCs n for all ΔT. The resulting three points of an airport that belong to ΔT values of 0 min, 5 min and 10 min are highlighted with different markers. Due to the proportionality between μ and n all points of an airport are located on a straight line passing through the origin. The gradient of this line decreases with an increasing number of flights.

A dashed line connects the 0 min and the 5 min markers, whereas the 5 min and 10 min markers are connected by a solid line. IATA airport codes are used to label and assign each line to an airport. A list of all IATA codes used in this paper can be found in the appendix (Table 2). The length of these lines indicates how the potential of an airport to conduct simultaneous formation flight departures changes with increased time offsets. Furthermore, these plots allow comparisons between airports with regard to μ and n.

Scenario I – All formations

Figure 8 indicates that the potential to identify FCs varies a lot among the airports.

With 20940 and 19800 FCs DXB and LHR show by far the highest potential. However, at $\Delta T = 0$ min LHR shows the most FCs, whereas with increasing ΔT DXB shows the most FCs. With regard to μ, LHR remains ahead of DXB.

However, NRT shows the highest values of μ for all ΔT settings. With 398 scheduled flights HEL has less than 5 % of flights compared to DXB but is still below the Top 10 airports according to μ at $\Delta T = 10$ min. The μ value of HEL at $\Delta T = 0$ min is significantly lower than the μ value of all other airports in the plot.

Figure 8 shows a trend towards higher μ and n values at increasing numbers of scheduled flights. However, a large number of scheduled flights does not necessarily lead to high values of μ and n, because the distribution of flights with respect to the flight directions and to the departure times in the flight schedule is decisive to identify FCs. As an example, at $\Delta T = 5$ min FRA has almost the same μ value as HEL, although the number of flights differs by more than a factor of 9.

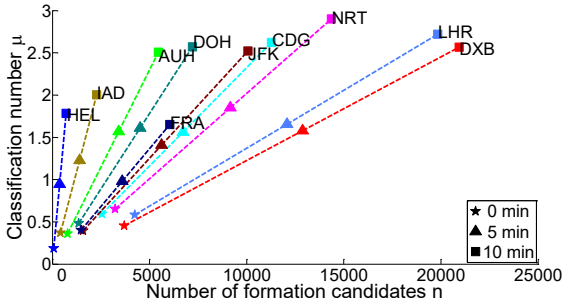

Figure 8: Comparison of the airport potential to conduct simultaneous formation flight departures depending on ΔT - Top 10 airports in terms of μ (Scenario I)

A comparison between JFK and FRA shows that the impact of increased ΔT on the potential of airports with similar numbers of scheduled flights (JFK: 3990, FRA: 3658) can be very different. μ and n are very similar at $\Delta T = 0$ min, whereas towards $\Delta T = 5$ min the increase of FCs at JFK compared to the increase of FCs at FRA almost differs by a factor of 2. JFK is a destination of

several airports in Europe and, therefore, JFK operates lots of flights towards Europe that have very similar routings, whereas the flights from Europe back to JFK are distributed between several airports in Europe. Thus, one reason leading to these differences can be identified in the high airport density in Europe.
Although Figure 8 does not explicitly include this information, it is interesting to note that seven of the presented airports (CDG, DOH, DXB, FRA, JFK, LHR, and NRT) are listed in the Top 10 ranking in terms of μ and n for all ΔT.

Scenario II – Common destination

In this scenario, especially at the airports with many scheduled flights, μ is drastically reduced. As a result only NRT, JFK, and HEL remain among the Top 10 airports according to μ as presented in Figure 9. It must be noted that the scaling of the axes is not the same as in Figure 8.
With 1300 FCs, NRT has by far the largest number of FCs with common destinations. LRM shows the highest values of μ. Increasing ΔT does not change the potential of LRM and DZA and results in 3 overlapping points each.
At $\Delta T = 0$ min BGI and HEL show no FCs, but as ΔT increases at both airports FCs can be identified. The number of FCs at BGI increases to 42 at an increase of ΔT from 0 min to 5 min and is constant at further increase, whereas the number of FCs at HEL increases in 2 steps from 0 to 12 and from 12 to 62 candidates. The big difference with respect to μ results from the fact that BGI operates less than 20 % of the flights compared to HEL. As it can be seen at the example of HEL, the increase of ΔT from 0 min to 5 min and from 5 min to 10 min affects the number of FCs to a varying extent. At KIX, the number of FCs increases from 80 to 84 at the first increase of ΔT and from 84 to 230 at the second increase, whereas at SHA the effect is opposite. 576 new candidates are identified by means of increasing ΔT from 0 min to 5 min, whereas further increase of ΔT adds only 40 new candidates.

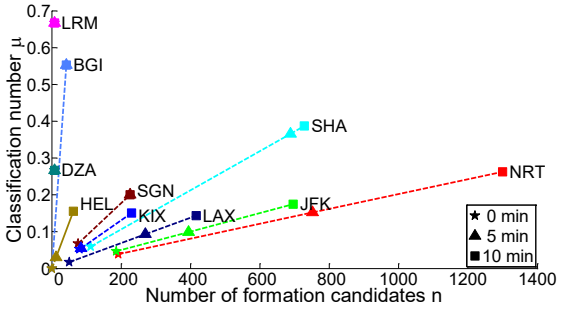

Figure 9: Comparison of the airport potential to conduct simultaneous formation flight departures depending on ΔT - Top 10 airports in terms of μ (Scenario II)

Scenario III – Star Alliance

As illustrated in Figure 10, the potential to identify FCs in this scenario is significantly decreased compared to scenario I. The maximum number of FCs is decreased from 20940 (cf. Figure 8) to 4432 and also the maximum value of μ is reduced to 1.05. At $\Delta T = 10$ min four airports (LIS, IAD, IST, and FRA) have a classification number around one. Thus, the number of FCs corresponds to the number of flights, although not every flight is assigned to a formation, because, for example, at IST or SIN some flights are assigned to formations with 8 other flights. As it can be seen in Figure 10, SIN and FRA are always on the first and second position in the ranking according to n, whereas LIS is always leading according to μ. Furthermore, it is interesting to note that at every ΔT FRA, IAD, IST, SIN, and ZRH are among the Top 10 airports according to μ and n, whereas NRT and BKK with almost 5000 scheduled flights each are only among the Top 10 airports according to n for all ΔT. The ΔT filter settings affect the potential to identify FCs at these airports in different manners. BKK shows more FCs at $\Delta T = 0$ min. But increasing ΔT by only 5 min allows NRT to increase n by almost as many new candidates as BKK can increase n when increasing ΔT by 10 min. NRT is the only airport among the Top 10 airports with respect to μ in all scenarios.
It is also interesting to note that at ΔT of 0 min and 5 min LHR is with 250 and 600 FCs among the Top 10 airports according to n, although it is not the home base of one of the alliance member airlines.

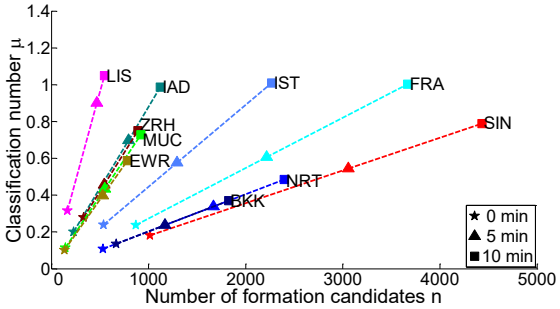

Figure 10: Comparison of the airport potential to conduct simultaneous formation flight departures depending on ΔT - Top 10 airports in terms of μ (Scenario III)

4.3. Airport potential according to fuel savings

This chapter deals with the airport potential with respect to fuel savings. Figure 11, Figure 12, and Figure 14 present the estimated fuel savings of the Top 15 airports according to the number of formations in the formation flight schedule (N). Besides the cumulated fuel savings of each airport ΔF_{ap}, the bar chart presents the number of formations N. Thus, the direct comparison between ΔF_{ap} (red bar) and N (blue bar) allows an estimation of the average efficiency of formations compared to other airports. The airports are sorted from left to right according to N in descending order.

Scenario I – All formations

As shown in Figure 11, LHR and DXB clearly have the highest fuel saving potential with estimated fuel savings of 19700 t and 18900 t. These in comparison to the third position (SIN) by almost a factor 1.9 higher fuel savings result from a significantly higher number of formations in the formation flight schedule compared to all other airports. This gap also exists in the number of FCs as depicted in Figure 8. The difference between the number of FCs of LHR and the next airport in the ranking (NRT) is almost 5500 candidates. The formation flight schedules of LHR and DXB count 2106 and 2087 formations. These values correspond to approximately 10 % of the FCs each. The remaining 90 % of the FCs are not considered, because they are either inefficient or at least one of the formation members is assigned to multiple formations, which required to choose the best formation sets. In general, it can be seen that the number of formations in the formation flight schedule corresponds to the number of FCs. Thus, the Top 10 airports according to n are all

ranked in the Top 15 according to N, although the order has changed, because the percentage of FCs considered in the formation flight schedule varies a lot among all airports. Among the airports mentioned in Figure 11, DOH and AUH have the smallest percentage of 9.1 % and 9.0 %, whereas PVG and PEK show the highest percentage of 23.3 % and 20.4 %. Although a larger candidate pool may lead to more promising formations in the formation flight schedule, μ is not suitable as an indicator of the efficiency of formations at an airport, because the number of assignments to different formations varies a lot among all flights. Furthermore, the efficiency depends on the flight routes and aircraft types, because the fuel savings are mainly affected by detours, the joint flight time and the aircraft mass.

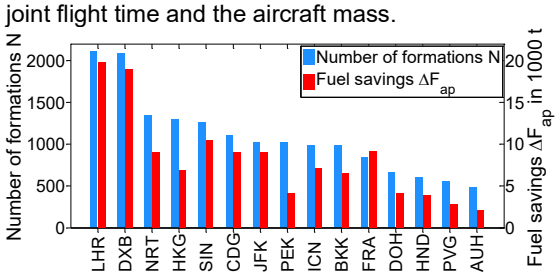

Figure 11: Airport potential in terms of fuel savings (red) - Top 15 airports in terms of N (blue) (Scenario I)

It is interesting to note that the fuel savings assigned to FRA and NRT are of the same magnitude, but the number of formations varies by almost 500. Thus, it can be concluded that the formations at FRA are more efficient than those at NRT. Reasons leading to a higher efficiency are discussed in scenarios II and III. According to the fuel savings FRA is ranked at the fourth position behind SIN. The formations at PEK are least efficient.

Scenario II – Common destination

Figure 12 shows that SHA has very inefficient formations, whereas the average efficiency of formations at DXB, JFK, LAX, LHR, and SIN with more than 10 t per formation turns out to be above average.

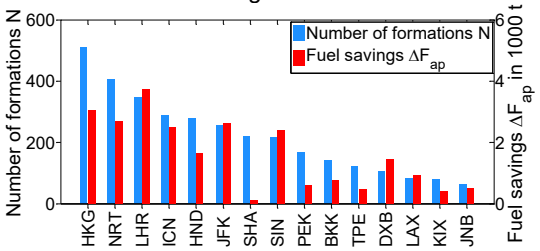

Figure 12: Airport potential in terms of fuel savings (red) - Top 15 airports in terms of N (blue) (Scenario II)

One reason can be identified in Figure 13, which shows the flight routes of all formations from LHR compared to those from SHA. Figure 13 shows that the average joint flight distance (green line) of all formations departing from SHA is significantly lower than the joint flight distance of formations departing from LHR. Because the fuel savings scale with the joint flight time, the estimated fuel savings at SHA turn out to be low. Further differences arise from different aircraft types, because the vorticity of the wake vortex and thus the fuel savings depend on the leader weight. The leader of more than half of the formations at DXB is an A380 and at LHR almost every third formation has an A380 on the leader position.

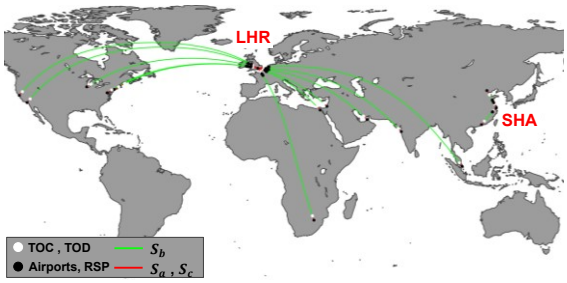

Figure 13: AWSE flight routes (LHR and SHA - Scenario II)

The HUB-airports HKG, HND, ICN, JFK, LHR, NRT, and SIN lead the ranking according to the fuel savings and the number of formations, because a higher number of flights increases the chance that two flights have the same destination. But it is interesting that FRA and CDG are not ranked among the Top 15 airports and DXB is ranked at position 12. Most of the ranked airports are located in Asia.

Scenario III – Star Alliance

The ranking with respect to the number of formations, as shown in Figure 14, is very similar to the ranking in Figure 10. The Top 5 airports according to their number of FCs in Figure 10 are all located on the leading positions according to their number of formations in the formation flight schedule, although the order has changed.

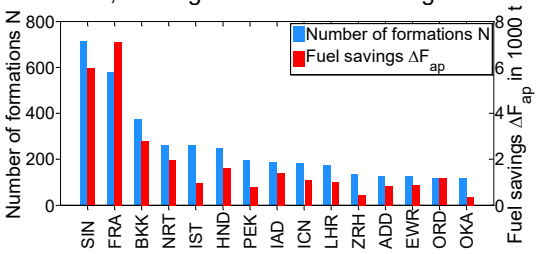

Figure 14: Airport potential in terms of fuel savings (red) - Top 15 airports in terms of N (blue) (Scenario III)

At NRT and IST each flight is, on average, assigned to 2.5 and 2.2 formations without consideration of both setups, whereas the average number of assigned formations at BKK is reduced to 1.6. Thus, the percentage of FCs considered in the formation flight schedule at BKK is almost twice as high as at NRT and IST. For this reason the position of BKK changes from the fifth position in the ranking according to the number of FCs (cf. Figure 10) to the third position in the ranking according to the number of formations in the formation flight schedule (Figure 14). With an average of only 1.4 formation assignments per flight, at HND more than 32 % of all FCs can be considered. SIN and FRA lead the ranking in Figure 14 with an average assignment to about 2 formations and a consideration rate of 16 % of all FCs each. As already shown in Figure 11, the formations at FRA are again more efficient than those at most other airports, although the number of formations with common destinations is rather small, as FRA is not listed among the Top 15 airports in scenario II (cf. Figure 12).

One reason may be the geographic location in Europe, which enables AWSE to very distant destinations in almost all flight directions, as it is indicated in the example of LHR in Figure 13. On the other hand, the formations at IST are less efficient. This results from the fact that most of these formations operate on shorter flight routes from Istanbul to

Europe or the Arab countries. Only a few formations have flight routes to Asia or the American East Coast. But it is interesting to note that all formations at IST are operated by a single airline (Turkish Airlines). Another interesting fact is that the big hub airports EWR, IAD, LHR, and NRT are among the Top 15 airports although they are not the home base of one of the members of Star Alliance. This shows the high potential of hub airports to conduct simultaneous formation flight departures.

4.4. Worldwide fuel saving potential

Table 1 lists the cumulated number of formations as well as the cumulated fuel savings and the average fuel savings of a formation for all three scenarios. These results indicate the high potential to reduce fuel consumptions in aviation by means of introducing AWSE from the same airport. Even by limiting the introduction of AWSE to formations with common destinations, which promise the least need for changes of the flight schedule, the estimated fuel savings are significant. Due to the elimination of detours, these formations are even more efficient. The average fuel savings in scenario III are comparable to those in scenario II, whereas the estimated worldwide fuel savings are slightly increased due to an increased number of formations. It is interesting to note that DXB and LHR are estimated to contribute more than 20 % to the worldwide fuel savings in scenario I.

Table 1: Worldwide fuel saving potential

Scenario	N_{tot}	ΔF_{tot} in 1000 t	$\frac{\Delta F_{tot}}{N_{tot}}$ in t
I	27352	187	6.8
II	4819	34	7.0
III	5264	37	7.0

5. CONCLUSION

The results presented above demonstrated that promising FCs can be identified at 159 of all 446 considered airports that operate long-haul flights. Furthermore, it was shown, that the number of FCs strongly varies with the airports and that an increase of the permitted time offset between scheduled departure times of formation members affects the number of FCs at an airport in different ways. In general, the more scheduled flights an airport has, the more FCs can be identified due to an increasing number of possible combinations, as the candidate pool of flights with similar flight directions scheduled within the same time interval ΔT grows. However, the individual distribution of flights in the flight schedule with respect to the flight directions and departure times is decisive to identify applicable FCs.

In order to assess the airport potential in terms of fuel savings, a formation flight schedule assigning each flight to only one formation was created. Analyzing these flight schedules revealed that due to multiple assignments the number of selected formations varies between 8 % and 50 %. The value of 50 % belongs to airports with less than 100 FCs and an average of about 260 scheduled flights, where the choice was made between both possible setups according to the aircraft position. However, it was found that these airports make only a small contribution to the worldwide fuel savings, because the Top 25 airports according to the number of formations in the formation flight schedule are estimated to achieve more than 80 % of the worldwide fuel savings. The fact that these Top 25 airports account for only about 73 % of all formations shows that the formations at these airports are also more efficient compared to the formations at the remaining airports due to the larger candidate pool. A larger candidate pool may also provide alternative formation members in the event of delay. It may, therefore, be concluded that there is a high fuel saving potential by conducting simultaneous formation flight departures especially at these hub airports.

Further studies need to analyze the impact of factors like wind and weather conditions affecting the flight routes and performance of AWSE and thus the achievable fuel savings. Moreover, the operational feasibility and economic efficiency taking into account additional flight times resulting from detours should be analyzed.

REFERENCES

[1] Wieselsberger, C., "Beitrag zur Erklärung des Winkelfluges einiger Zugvögel", *Zeitschrift für Flugtechnik und Motorluftschifffahrt*, Jahrgang V, Heft 15, pp. 225 – 229, 1914

[2] Lissaman, P. B. S., Shollenberger, C. A., "Formation Flight of Birds", *Science*, Vol. 168, pp. 1003-1005, 1970

[3] Hummel, D., "The Use of Aircraft Wakes to Achieve Power Reductions in Formation Flight", *AGARD Conference Proceedings 584*, Trondheim, Norway, pp. 36.1-36.13, 1996

[4] Beukenberg, M., Hummel, D., "Aerodynamics, Performance and Control of Airplanes in Formation Flight", Technische Universität Braunschweig, 1990, ICAS-90-5.9.3

[5] Vachon, M. J., Ray, R. J., Walsh, K. R., Ennix K., "F/A-18 Performance Benefits Measured During the Autonomous Formation Flight Project", *Atmospheric Flight Mechanics Conference*, 2003

[6] Pahle, J., Berger, D., Venti, M., Faber, J., Duggan, C., and Cardinal, K., "A Preliminary Flight Investigation of Formation Flight for Drag Reduction on the C-17 Aircraft", *Presentation at Atmospheric Flight Mechanics Conference*, 2011

[7] Visser, H. G., Santos, B. F., and Verhagen, C. M. A., "A Decentralized Approach to Formation Flight Routing", *ATRS World Conference*, Rhodes, Greece, 2016

[8] Xue, M., Hornby, G.S., "An Analysis of the Potential Savings from Using Formation Flight in the NAS", *AIAA Guidance, Navigation and Control Conference*, Minneapolis, Minnesota, 2012

[9] Bower, G. C., Flanzer, T. C., Kroo, I. M., "Formation Geometries and Route Optimization for Commercial Formation Flight", *27th AIAA Applied Aerodynamics Conference*, San Antonio, Texas, 2009

[10] Xu, J., Ning, A. S., Bower, G. C., Kroo, I. M., "Aircraft Route Optimization for Formation Flight", *AIAA Journal of Aircraft*, Vol. 51, pp. 490-501, 2014

[11] Kent, T. E., Richards, A. G., "A Geometric Approach to Optimal Routing for Commercial Formation Flight", *AIAA Guidance, Navigation and Control Conference*, Minneapolis, Minnesota, 2012

[12] Drews, K., "Identifikation und Modellierung ziviler Formationsflüge auf Basis von globalen Flugplandaten", Hamburg University of Applied Sciences (HAW Hamburg), Department of Automotive and Aeronautical Engineering, Master thesis, 2016

[13] Kent, T. E., Richards, A. G., "Accounting for the Effect of Ground Delay on Commercial Formation Flight", *UKACC International Conference on Control*, Loughborough, UK, 2014

[14] Marks, T., Linke, F., Gollnick, V., "Ein Ansatz zur Bewertung des Konzeptes von Formationsflügen ziviler Verkehrsflugzeuge im Lufttransportsystem", *62. Deutscher Luft- und Raumfahrt-Kongress*, 2013

[15] Sabre, Airport Data Intelligence, Database, Flight Schedule of October 2014

[16] Marks, T., Linke, F., Gollnick, V., "Entwicklung einer Methode zur vereinfachten Ermittlung von Leistungsmerkmalen ziviler Formationsflüge", *63. Deutscher Luft- und Raumfahrt-Kongress*, 2014

[17] Marks, T., "Modellansätze zur Bewertung von Formationsflügen im Lufttransportsystem", Ph.D. thesis, Hamburg University of Technology, Germany, 2019

[18] European Organisation for Safety of Air Navigation (EUROCONTROL), Aircraft Performance Model, Base of Aircraft Data Family 4 (BADA-4)

[19] IATA Economics, "Air Passenger Market Analysis", October 2014

[20] European Organisation for Safety of Air Navigation (EUROCONTROL), "ATM Lexicon – Calculated Take-Off Time", URL: https://ext.eurocontrol.int/lexicon/index.php/Calculated_Take-Off_Time [cited 21 July 2020]

[21] Mensen, H., "Handbuch der Luftfahrt", 2nd ed., Springer-Verlag, Berlin Heidelberg, 2013

[22] Khuloud, G., Mowaffaq, H., "The Fermat Point of a Spherical Triangle", *The Mathematical Gazette*, Vol. 80, no 489, pp. 561-564, November 1996

[23] Rooseleer, F., Treve, V., "RECAT-EU European Wake Turbulence Categorisation and Separation Minima on Approach and Departure", EUROCONTROL, 2015

[24] Mensen, H., "Planung, Anlage und Betrieb von Flugplätzen", 2nd ed. Springer-Verlag, Berlin Heidelberg, 2013

[25] Scheiderer, J., "Angewandte Flugleistung – Eine Einführung in die operationelle Flugleistung vom Start bis zur Landung", Springer-Verlag, Berlin Heidelberg, 2008

[26] Schmitz, G., "Konzepterstellung und Analyse des Formationsfluges ziviler Luftfahrzeuge beim Start von parallelen Startbahnen", RWTH Aachen University, Institute of Aerospace Systems, Master thesis, 2017

ACKNOWLEDGMENTS

The work presented in this paper is based on the results of the master thesis by Gregor Schmitz [26] and was part of the project FORMIC that was funded by the German Ministry of Economic Affairs and Energy (BMWi) under the National Aeronautical Research Program (LuFo) V-2 under the grant agreement no. 20E508A.

APPENDIX

Table 2: IATA Airport codes

IATA code	Name and location of the airport
ADD	Addis Ababa Bole Airport, Ethiopia
AUH	Abu Dhabi International Airport, United Arab Emirates
BGI	Bridgetown Grantley Adams International Airport, Barbados
BKK	Bangkok-Suvarnabhumi, Bangkok, Thailand
CDG	Paris Charles de Gaulle Airport, France
DOH	Doha Hamad International Airport, Qatar
DXB	Dubai International Airport, United Arab Emirates
DZA	Dzaoudzi Pamandzi International Airport, Mayotte
EWR	New York Newark Liberty International Airport, USA
FRA	Frankfurt Airport, Germany
HEL	Helsinki Vantaa Airport, Finland
HKG	Hong Kong International Airport, Hong Kong
HND	Tokyo Haneda International Airport, Japan
IAD	Washington Dulles International Airport, USA
ICN	Seoul Incheon International Airport, South Korea
IST	Istanbul Airport, Turkey
JFK	New York John F. Kennedy International Airport, USA
JNB	Johannesburg O.R. Tambo International Airport
KIX	Osaka Kansai International Airport, Japan
LAX	Los Angeles International Airport, USA
LHR	London Heathrow Airport, United Kingdom
LIS	Lisbon Humberto Delgado Airport, Portugal
LRM	La Romana International Airport, Dominican Republic
MUC	Munich Airport, Germany
NRT	Tokyo Narita International Airport, Japan
OKA	Naha Airport, Japan
ORD	Chicago O'Hare International Airport, USA
PEK	Beijing Capital International Airport, China
PVG	Shanghai Pudong International Airport, China
SGN	Ho Chi Minh City International Airport, Vietnam
SHA	Shanghai Hongqiao International Airport, China
SIN	Singapore Changi Airport, Singapore
TPE	Taiwan Taoyuan International Airport, Taiwan